Improved Methodology for Power Transformer Loss Evaluation: Algorithm Refinement and Resonance Risk Analysis

Mantas Plienis *, Tomas Deveikis, Audrius Jonaitis [ID], Saulius Gudžius, Inga Konstantinavičiūtė and Donata Putnaitė

Department of Electric Power Systems, Kaunas University of Technology, Studentu Str. 48, LT-51367 Kaunas, Lithuania; tomas.deveikis@ktu.lt (T.D.); audrius.jonaitis@ktu.lt (A.J.); saulius.gudzius@ktu.lt (S.G.); inga.konstantinaviciute@ktu.lt (I.K.); donata.putnaite@ktu.lt (D.P.)
* Correspondence: mantas.plienis@ktu.edu; Tel.: +370-638-42872

Abstract: The decline in power quality within electrical networks is adversely impacting the energy efficiency and safety of transmission elements. The growing prevalence of power electronics has elevated harmonic levels in the grid to an extent where their significance cannot be overlooked. Additionally, the increasing integration of renewable energy sources introduces heightened fluctuations, rendering the prediction and simulation of working modes more challenging. This paper presents an improved algorithm for calculating power transformer losses attributed to harmonics, with a comprehensive validation against simulation results obtained from the Power Factory application and real-world measurements. The advantages of the algorithm are that all evaluations are performed in real-time based on single-point measurements, and the algorithm was easy to implement in a Programmable Logic Controller (PLC). This allows us to receive the exchange of information to energy monitoring systems (EMSs) or with Power factor Correction Units (PFCUs) and control it. To facilitate a more intuitive understanding and visualization of potential hazardous scenarios related to resonance, an extra Dijkstra algorithm was implemented. This augmentation enables the identification of conditions, wherein certain branches exhibit lower resistance than the grid connection point, indicating a heightened risk of resonance and the presence of highly distorted currents. Recognizing that monitoring alone does not inherently contribute to increased energy efficiency, the algorithm was further expanded to assess transformer losses across a spectrum of Power Factory Correction Units power levels. Additionally, a command from a PLC to a PFCU can now be initiated to change the capacitance level and near-resonance working mode. These advancements collectively contribute to a more robust and versatile methodology for evaluating power transformer losses, offering enhanced accuracy and the ability to visualize potentially critical resonance scenarios.

Keywords: power transformer losses; energy efficiency; resonance hazard; harmonics

1. Introduction

The global transition to renewable energy sources has witnessed a remarkable rise in recent decades, driven by mounting environmental concerns and the pursuit of sustainable energy solutions [1]. Solar photovoltaic systems, wind turbines, and other power electronic technologies have emerged as cornerstones of the green energy revolution. In 2022, wind and solar power generated 22% of the EU's electricity, overtaking gas for the first time [2]. Additionally, in modern industrial power supply systems, there has been a significant increase in the installed capacity of nonlinear electric sources [3], and total capacity in Europe, only in photovoltaics, has increased by 25% from 167.5 GW in 2021 to 208.9 GW 2022 [4]. However, as these sources are integrated into existing electrical grids, complex challenges for power quality appear [5].

The rise of renewable energy sources, often characterized by variable [6] and nonlinear power generation profiles, has brought about a significant transformation in power

grids [7]. Traditional electrical networks, designed for steady-state and sinusoidal operation, are now contending with a new set of operational dynamics [8]. These dynamics encompass fluctuations in energy production, voltage irregularities, and a growing prevalence of harmonic distortions [9]. Recently, the widespread use of power electronic systems increased in magnitude [10], therefore it has become a key issue in installations [11]. Harmonic distortion not only poses threats to the operational lifespan of equipment such as power transformers but also leads to energy losses that impact economic viability [12].

This article delves into the intricate interplay between harmonic distortion and energy losses, with a particular focus on the consequences of harmonic resonance and decreased efficiency of power transformers in power distribution systems. Energy losses are a fundamental issue in the energy sector [13]. It is imperative to increase energy efficiency constantly [14]. This pursuit is not only beneficial for both industry and the climate [15], but it is also indispensable, as adept energy management can help to reduce costs and increase profit [16]. Real-time monitoring and recording of energy consumption data can aid in identifying important energy losses in a facility [17] and allow the implementation of various energy-saving practices to reach up to 8% in energy efficiency [18]. Nevertheless, energy monitoring itself does not save energy [19] because data must be not only collected, but also conclusions should be made on how to improve, and this process is significantly more challenging in the presence of harmonics [20].

In the domain of transformer losses attributed to harmonic distortion, the majority of analyses are in alignment with the recommendations outlined in IEEE Std C57.110-2018 recommendations [21–23]. Building upon similar technological foundations, article [24] uses a comparable methodology to evaluate the maximum loading capacity of transformers in the presence of harmonic influences. Simulations hold a significant role in scientific literature and are indispensable. In the context of transformer losses, it is essential to consider both simulations and real measurements for a comprehensive understanding. Comparisons of transformer losses have been conducted through real measurements in relation to the EMTP-RV model [25,26] and with the Matlab/Simulink model [27]. Additionally, simulations using ETAP-Etrax Software have been employed for a big railway system in the article [28]. Even though the finite element method (FEM) is an effective technique [29,30] for handling the distribution of losses in various metallic structures [31], it takes a lot of time and processing capacity [32].

Currently, studies on power transformer losses due to harmonics are mainly with simulated data [33] or historical data [34]. The disadvantage of those methods are calculations and evaluations, which are performed in one operating point [35]. The drawback of these methods lies in the fact that calculations and evaluations are conducted at a single operating point, whereas operating points and the loading profile are subject to constant change. The increasing prevalence of renewables further amplifies their substantial influence in this regard [36]. The static load model is suitable for the steady state, as it does not involve load dynamics [37], and this gives errors due to discrete time, or the wide usage is limited.

The most precise assessment of power transformer losses can be achieved through measurements [38], particularly in controlled laboratory conditions [39]. However, translating this methodology into the real industrial environment proves to be more costly due to the need for duplicate measurement devices and poses complexities, primarily attributed to the utilization of medium voltage measurement equipment. The goals of lowering energy waste and increasing awareness of energy efficiency can only be achieved by measuring and controlling energy consumption [40]. Internet of Things technologies are currently supporting these efforts [41,42] by making a vast amount of data readily available for analysis [43]. In article [44], energy efficiency was improved only by gathering data with a monitoring system and then identifying energy losses. To add in different articles [45], it was presented that giving enterprises a tool to assess and comprehend their actual energy management capabilities is vital to find areas where improvements can be made.

Monitoring alone is insufficient, and it is necessary to detect abnormal energy consumption data in real-time [46]. In article [47], real-time monitoring was presented ac-

cording to IEEE Std C57.110-2018 [48], which evaluates the increase in the temperature of the transformer due to harmonic distortion. Publication [49] presented monitoring of insulation ageing, and neural networks were used for evaluation in publication [50]. To approach assessment of losses in sufficient manner, it is important to develop universal and efficient algorithmic methods [51] in terms of implementation convenience as well as acceptable computational complexity [52]. The significance of this study lies in its potential to improve energy monitoring [53] systems with a real-time algorithm to mitigate risks promptly. Real-time experiments validate that the proposed method is effective and has good application prospects [46]. For this reason, article [54] presented a simplified algorithm implementation in the programmable logic controller, which resulted in sufficient calculation precision compared to the measurement. During the experiment, which was presented in article [54], it was noticed that the power factor correction unit (PFCU) decreased efficiency due to ongoing series resonance compared to the state where the PFCU was disconnected. This condition is serious not only because of the derating of the transformer [55], but it also can lead to explosions of the capacitors [56]. The algorithm must not only calculate the transformer's losses due to harmonics but also evaluate harmful conditions such as resonance.

This paper is organized as follows: Section 2 describes of the procedure of calculating resonance frequencies, additional transformer losses due to harmonic presence, and the equation explanations with the schemes for evaluating resistances versus frequency. The results of the calculations and comparison to simulations are provided in Section 3. The paper ends with the conclusion section, where the results and future work are presented.

2. Materials and Methods

One of the vital issues in industrial and distribution power systems is increasing the use of nonlinear loads and increasing power of inverter-based distributed generation, which leads to higher harmonic disturbances in a grid [57]. Harmonic currents in the inverter are generated because of usage pulse-width modulation [58]. In power systems, harmonics are generally managed by adding filters, circuit detuning, and usage of phase-shifting transformers [59] or inverters with harmonic current compensation compatibility [60].

The power transformer, the main equipment in the utility network [61], plays a very important role because the failure of the transformer can cause serious power outages [20]. Under normal operating conditions, transformers are typically not a significant source of harmonics in power systems. Despite historically being the first cause of harmonics, their relationship between primary voltage and currents follows a non-linear magnetization curve, experiencing distortion if located within saturation regions [62]. This distortion affects the magnetizing current, but the impact on harmonics is minimal even with a large number of transformers operating [63]. In addition to the fact that the transformer is a harmonic source itself, the transformer's efficiency can drop drastically while supplying non-linear loads.

Normally in industrial plants in parallel to transformers, PFCUs are installed, which consist of capacitor banks. The capacitors are not a source of harmonic current but can have the effect of magnifying such currents [64]. Capacitor banks in industrial power systems are mainly used for power factor correction purposes. A PFCU with installed capacitor banks is predominantly employed in reactive power compensation technology owing to its highly cost-effective pricing. In various applications of a PFCU within a power system network, the interaction between the inductance of a transformer and the capacitance of a PFCU introduces a noteworthy consideration. Specifically, due to the combinations of these elements, a frequency is invariably present at which the capacitance aligns in either parallel or series resonance with the transformer or the grid. When this condition appears on, or close to, cases of series resonance, the increased harmonic currents will circulate through the power transformer between the utility network and the power factor equipment, causing additional losses to the system [65]. Harmonic resonance is a key concern in the power quality analysis of industrial power systems. This event can threaten the reliability of the

system and can cause significant issues in industrial plants [66]. Under series resonance conditions, there is an augmentation of current through the capacitor bank, leading to supplementary losses. Consequently, this can give rise to adverse effects, including circuit breaker tripping or fuses blowing. Additionally, physicochemical processes occurring in the dielectric may result in accelerated ageing of the insulation, contributing to heightened service costs, permanent damage, and related complications [67].

If the system is considered from the point of view of the distribution network, then the power transformer is in series resonance with the power factor correction unit [68]. The resonant frequency f_{res} can be found with Equation (1).

$$f_{res} = f_1 \times \sqrt{\frac{S_r}{U_k \times Q_C}} \tag{1}$$

where Q_C is the reactive power of the capacitor, S_r is the apparent rated power of the transformer, and U_k is the impedance of the voltage transformer in percent.

In article [54], its algorithm to evaluate the effect of harmonics on a power transformer was implemented in PLC. This implementation allowed to measure losses and efficiency of the power transformer in real-time and was tested in real conditions, and the results were compared to the measurements of the MV side of the transformer. Observations during the experiment revealed that ongoing resonance has a more pronounced impact on the efficiency of the transformer compared to power factor correction. In certain scenarios, it was determined that it might be more advantageous not to compensate reactive power than to engage in compensation while neglecting the associated risk of resonance. To create an algorithm, firstly, key parameters of the transformer must be calculated. The copper losses of the power transformer P_{I^2R} in kW are calculated according to Equation (2).

$$P_{I^2R} = K\left(I_{1f}^2 \times R_1 + I_{2f}^2 \times R_2\right) \tag{2}$$

where K is the constant coefficient (for a single-phase transformer, K equals 1; for a three-phase transformer, K equals 1.5), R_1 and R_2 are the resistances of primary and secondary windings, respectively, and I_{1f} and I_{2f} are the rated current of primary and secondary windings, respectively. When the copper losses of the power transformer are known, the nominal stray losses P_{TSL-N} are found according to Equation (3).

$$P_{TSL-N} = P_{LL} - P_{I^2R} \tag{3}$$

where P_{LL} is the rated load losses of the transformer.

According to article [48], the ratio of total stray losses for the oil-filled power transformer, equal to 1000 kVA of power, is 50 percent for the nominal Eddy current losses P_{EC-N} in kW and 50 percent for other stray losses P_{OTSL} in kW; these can be calculated according to Equations (4) and (5).

$$P_{EC-N} = P_{TSL-N} \times 0.5 \tag{4}$$

$$P_{OTSL} = P_{TSL-N} \times 0.5 \tag{5}$$

For distorted currents, RMS of current I_{pu} in proportional units is calculated according to Equation (6).

$$I_{pu} = \sqrt{\sum_{h=1}^{h=hmax} I_h^2} \tag{6}$$

where h is the harmonic order, h_{max} is the highest order of measured harmonic, and I_h is the per unit rms current at harmonic h. The harmonic loss factor of Eddy current losses F_{HL-STR} is calculated according to Equation (7).

$$F_{HL} = \frac{\sum_{h=1}^{h=hmax} I_h^2 h^2}{\sum_{h=1}^{h=hmax} I_h^2} \tag{7}$$

The harmonic loss factor of other stray losses is F_{HL-STR} calculated according to Equation (8).

$$F_{HL-STR} = \frac{\sum_{h=1}^{h=hmax} \left[\frac{I_h}{I}\right]^2 h^{0.8}}{\sum_{h=1}^{h=hmax} \left[\frac{I_h}{I}\right]^2} \tag{8}$$

The loading of the transformer P_{LLpu} per unit is calculated according to Equation (9).

$$P_{LLpu} = \frac{S_L}{S_N}^2 \times I_{pu}^2 \tag{9}$$

where S_L is the apparent power of the load in kVA, and S_N is the apparent power of the power transformer in kVA. The losses of the power transformer P_{TL} in W with given harmonic content can be calculated according to Equation (10).

$$P_{TL} = P_0 + (P_{I^2R} \times P_{LLpu}) + (P_{EC-N} \times P_{LLpu} \times F_{HL}) + (P_{OSL} \times P_{LLpu} \times F_{HL-STR}) \tag{10}$$

where P_0 is the idle losses of the transformer. The active power load P_{MV} in kW on the MV side is calculated according to Equation (11).

$$P_{MV} = P_{TL} + P_L \tag{11}$$

where P_L represents the active load of the transformer.

To implement this algorithm, the PLC is needed to do frequency sweep calculations in real-time. To calculate the parameters for the resonance, we need to calculate the reactive resistances of the power factor correction unit and the power transformer. Considering what is presented in Figure 1, a simple system of an industrial distribution network, which has a transformer and a PFCU, the MV busbars are connected to the grid via an HV transformer.
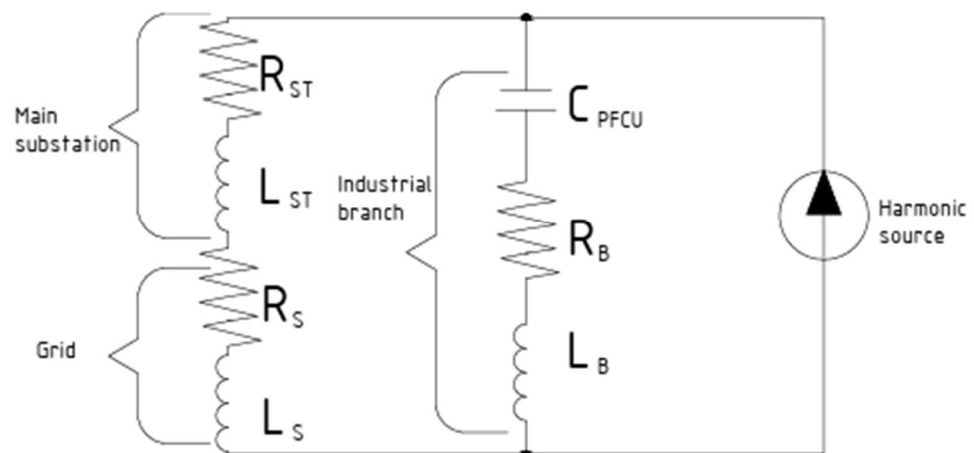

Figure 1. A simple industrial system consisting of the industrial branch with a transformer and a PFCU.

If active resistance is neglected, the equivalent impedance Z_z can be calculated according to Equation (12).

$$Z_z = \cfrac{1}{\cfrac{1}{(L_S+L_{ST)} \times 2\pi f} + \cfrac{1}{L_{TR} \times 2\pi f - \frac{1}{C_{PFCU} \times 2\pi f}}} \tag{12}$$

where L_s is the inductance of the system, L_{ST} is the inductance of the HV transformer, L_{TR} is the inductance of the MV transformer, f is the frequency, and C_{PFCU} is the capacitance of the power factor correction unit.

To calculate different scenarios of the PLC, there is a need to know how current injections in industrial branches are changed due to different capacitances of the PFCU. First Kirchhoff's law states that the current flowing into a node (or a junction) must be equal to the current flowing out of it. In Figure 2, it is presented that the current injected into the distribution busbar is divided into the grid and to another industrial branch.
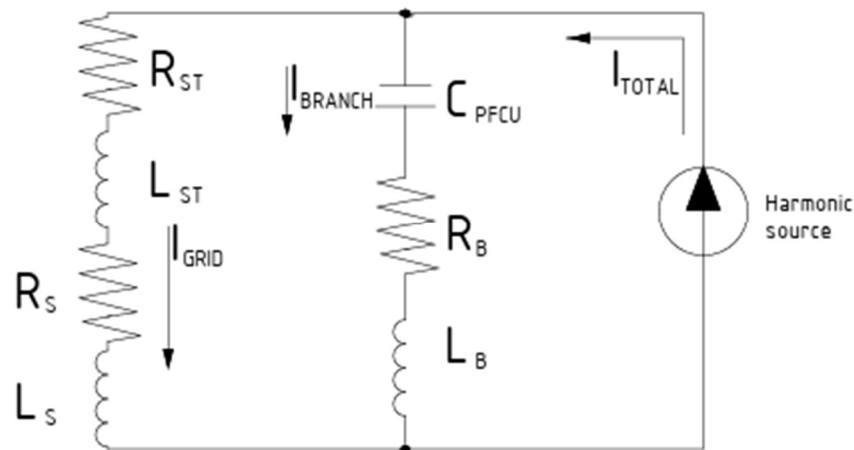

Figure 2. Equivalent scheme to represent harmonic currents flow.

When the resistance values of the system are known, the ratio of current absorbed by the industrial branch $I_{1\%}$ and grid can be calculated according to Equation (13) if the total injected current I_T is known.

$$I_{1\%} = 100 \times \cfrac{I_T \times \sqrt{(R_S + R_{ST})^2 + ((L_S + L_{ST}) \times 2\pi f)^2}}{\cfrac{\sqrt{(R_S+R_{ST})^2+((L_S+L_{ST}) \times 2\pi f)^2} + \sqrt{R_{TR}^2 + (\frac{1}{L_{TR} \times 2\pi f - \frac{1}{C_{PFCU} \times 2\pi f}})^2}}{I_T}} \tag{13}$$

where R_S is the resistance of the network, R_{ST} resistance of the HV transformer, and R_{TR} is the resistance of the industrial branch transformer.

One of the benefits of algorithm was listed as the possibility to use it only with the measurements on the low voltage side, which is cheaper and safer. For this reason, Equation (14) can be used to calculate the harmonic current flown in MV busbars I_T in case the measurements are only available on the 0.4 kV side (I_B).

$$I_T = \cfrac{I_B \times \sqrt{(R_S + R_{ST})^2 + ((L_S + L_{ST}) \times 2\pi f)^2} + \sqrt{R_{TR}^2 + (\frac{1}{L_{TR} \times 2\pi f - \frac{1}{C_{PFCU} \times 2\pi f}})^2}}{\sqrt{(R_S + R_{ST})^2 + ((L_S + L_{ST}) \times 2\pi f)^2}} \tag{14}$$

Equations (13) and (14) can be represented in an equivalent scheme of the network, which is provided in Figure 3.
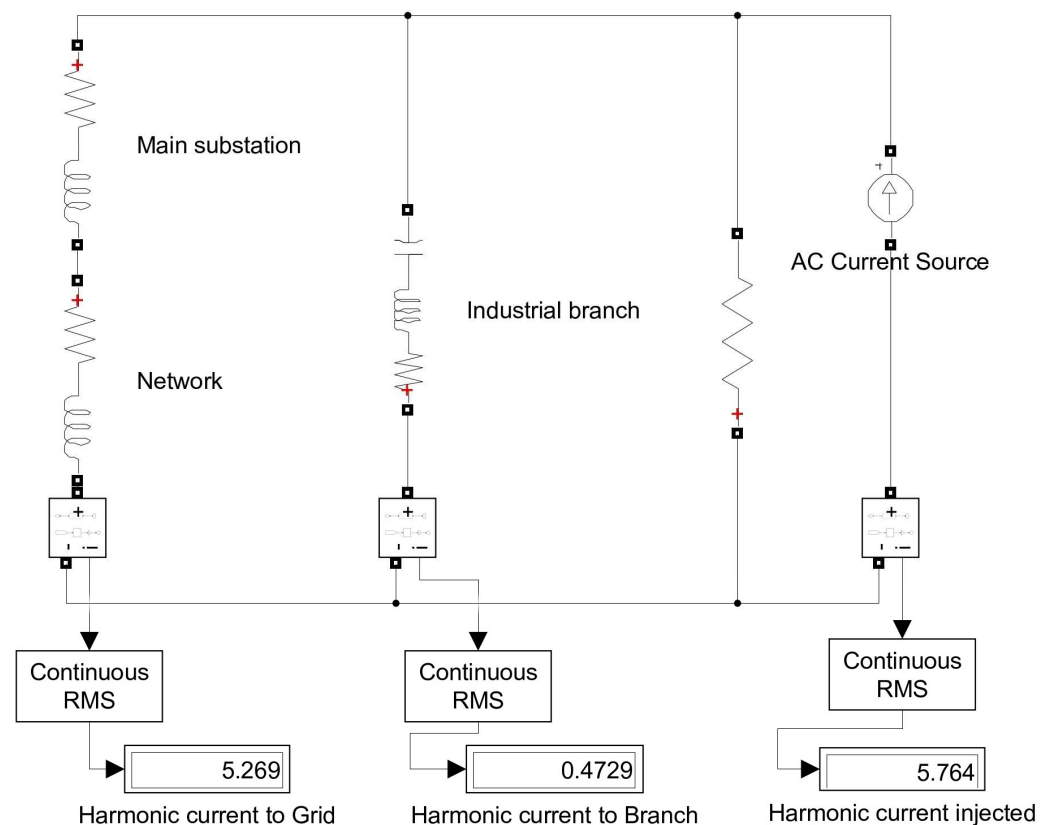
Figure 3. Equivalent scheme to represent harmonic currents flow values.

Equations (13) and (14) allow us to recalculate the current drawn from the MV grid to the industrial plant branch with different powers of the PFCU and to find the correlation in which PFCU mode is best for the power transformer loss, considering not only displacement power factor but harmonic distortion too.

Harmonic currents will tend to flow into the system capacitance [69], or, in the case of resonance, relatively higher currents can flow to the branch that has the smallest resistance. For quick evaluation of the possible current harmonic path, the Dijkstra algorithm can be used. The algorithm can be used for finding the shortest paths from one vertex to another in a weighted graph with non-negative weights. In this scenario, the weight of the path is equal to the absolute impedance of the branch. The Dijkstra algorithm was added to the algorithm for a more user-friendly understanding of impedance relationships and harmonic current flow. In the test device, the algorithm is used four times to calculate harmonic current flow in the following frequencies: 250 Hz, 350 Hz, 550 Hz, and 650 Hz. Figure 4 shows a simplified equivalent scheme for the usage of the Dijkstra algorithm. For harmonic current to flow from point A to point B, there are two possible ways, with different resistances. This algorithm calculates resistance for desired frequencies, and, in the case of resonance, the path through Z_{TR1} will be shown; this means that the transformer is exposed to higher current harmonics.

The Dijkstra algorithm's implementation allows us to monitor frequency sweep changes in bigger systems and detect dangerous resonance scenarios in real time.
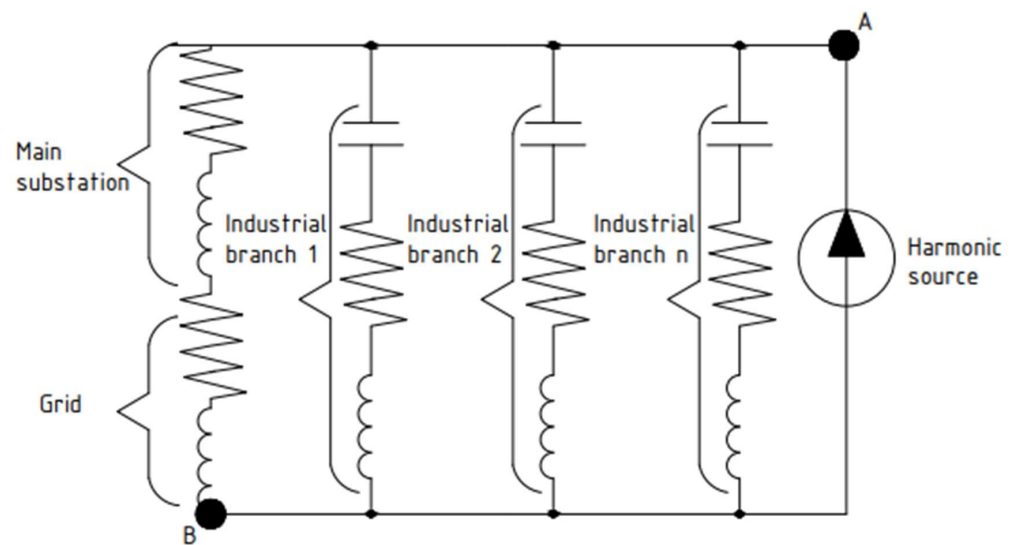
Figure 4. Equivalent scheme to represent logic for Dijkstra algorithm.

3. Results

To check the accuracy of implemented the algorithm, the same conditions as those presented in article [54] were modeled in a Power Factory environment. The model consisted of two MV voltage connection points, which were the first branch representing the consumer with the transformer and PFCU and the second branch representing the current distortion source. The model of the Power Factory environment is shown in Figure 5.
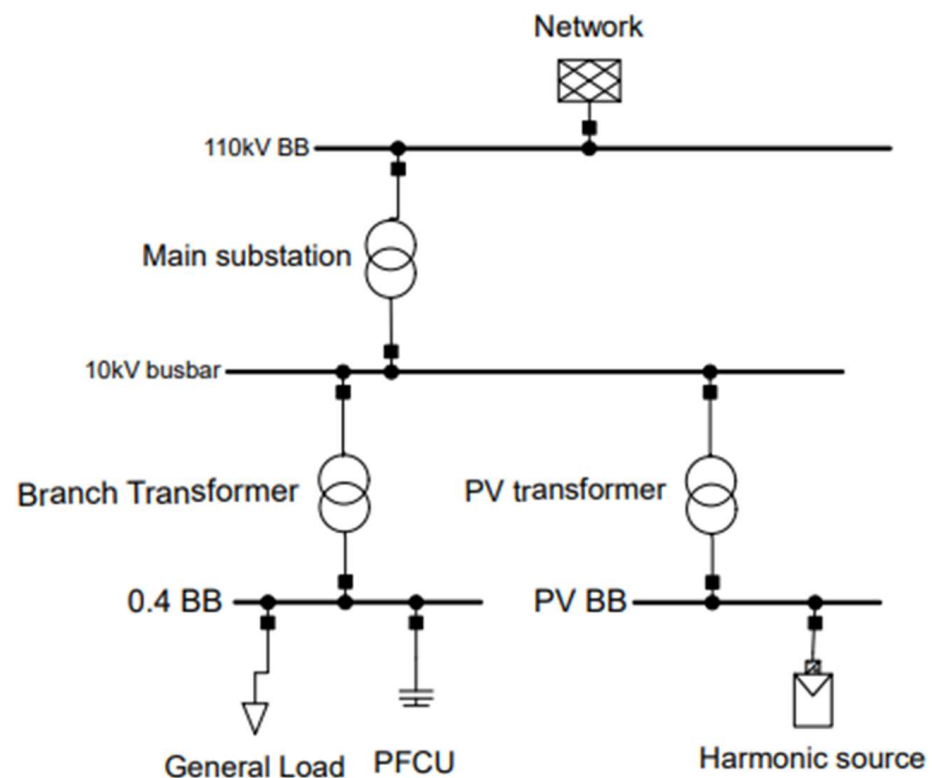

Figure 5. Model in the Power Factory environment.

The input data for the simulation are listed in Table 1.

Table 1. Input data for the simulation.

Load on LV Side				Order of the Harmonics and Value in %								
Active Power P_L, kW	Reactive Power Load, Q_L	Apparent Power S_L, kVA	Power of PFC Q_c, kVAr	3	5	7	9	11	13	15	17	19
181.56	140	182.73	120	0	1.76	1.68	0	7.03	0	0	0	0

Table 2 provides the results of the real measurement, the calculation with the PLC, and the simulation with the Power Factory.

**Table 2.** Comparison between real measurements, calculations, and simulation.

	Measured in MV	Calculations	Simulated with Power Factory
Losses calculated, kW		3.076	3.12
Load LV, kW		181.56	181.56
Load measured MV, kW	184.7		
Sum	184.7	184.636	184.68
Relative error to measurement, %	-	0.0347	0.0108
Relative error to simulation	−0.011	0.024	-

It was noticed that additional iterations were needed to improve the accuracy of the algorithm because the transformer loading increased due to the harmonics losses. The results after the improved algorithm are listed in Table 3.

Table 3. Comparison after additional iteration added to the algorithm.

	Measured in MV	Calculations	Simulated with PF	Calculations with Additional Iteration
Losses calculated, kW		3.076	3.12	3.091
Load LV, kW		181.56	181.56	181.56
Load measured MV, kW	184.7			
Sum	184.7	184.636	184.68	184.651
Relative error to measurement, %		0.0347	0.0108	0.0265
Relative error to simulation	−0.011	0.024		0.016

When the model was tested, it allowed us to do the simulations with more various scenarios, such as different powers in the PFCUs. Figure 6 shows us that, due to resonance even with a relatively small THD of current, the most efficient scenario does not fully compensate for the reactive power. For this reason, it is useful to make calculations in real-time, and PLC allows for the possibility to receive real data from the PFCU; in the case of a resonance scenario, the PLC can send a command to the PFC to change its power.
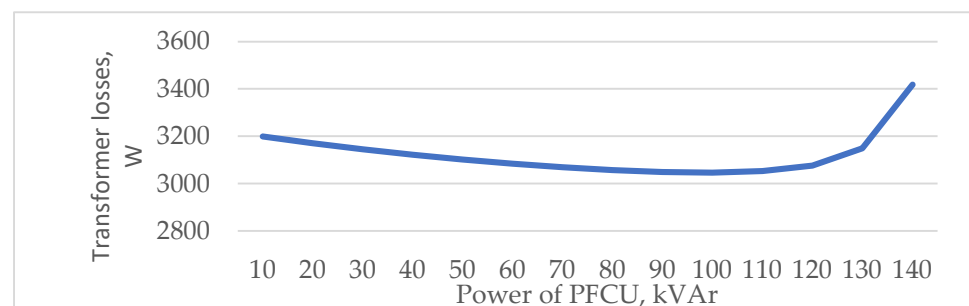
Figure 6. Changes in the transformer losses due to different power of PFCU.

To evaluate the resistances and frequency sweep of the system's simplified model, Power Factory was used. A simplified model with a neglected load is provided in Figure 7.
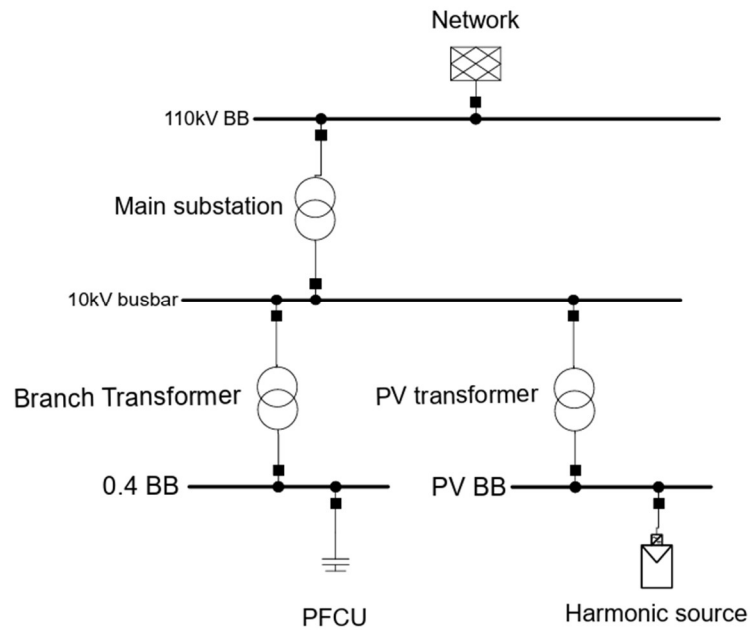

Figure 7. Model used to evaluate resistances and harmonic flow.

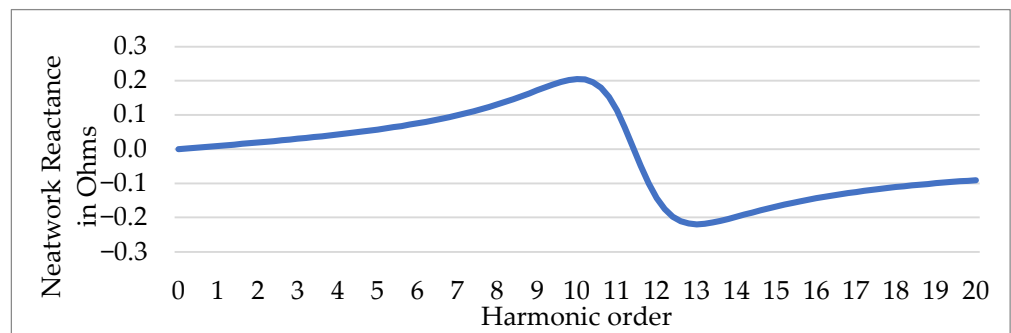In Figure 8, network reactance results according to the frequency sweep in the Power Factory are shown.

Figure 8. Results of frequency sweep in the Power Factory application.

According to Equation (13), the current ratios between branches are provided in Figure 9. It can be seen the harmonic current to branch is exceeding the harmonic current to grid only in the resonance scenario.
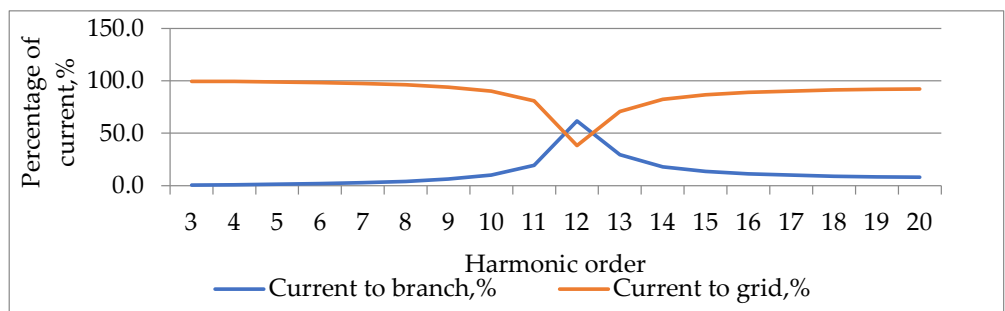

Figure 9. Division of the currents to industrial branch and grid.

The results of Equation (14), recalculating the total distorted current in MV busbars, are represented in Table 4.

Table 4. Calculated total distorted current injected to MV busbars.

	I_B, A	I_T, A
5th harmonic current	0.19	18.0
7th harmonic current	0.18	7.2
11th harmonic current	0.77	4.0
13th harmonic current	0	0

When the currents circulating in MV busbars are known, it allows us to recalculate the current drawn by the branch in different power of PFCU I_B'. The results are provided in Table 5.

Table 5. Calculated total distorted current injected to industrial branch with different powers of PFCU.

Power of PFCU, kVAr	Calculated Current of I_B', A			
	5th Harmonic	7th Harmonic	11th Harmonic	13th Harmonic
10	0.01	0.01	0.02	0
20	0.03	0.02	0.03	0
30	0.04	0.03	0.05	0
40	0.06	0.05	0.08	0
50	0.07	0.06	0.11	0
60	0.09	0.07	0.14	0
70	0.10	0.09	0.18	0
80	0.12	0.11	0.24	0
90	0.14	0.12	0.31	0
100	0.15	0.14	0.41	0
110	0.17	0.16	0.55	0
120	0.19	0.18	0.77	0
130	0.21	0.21	1.15	0
140	0.23	0.23	2.00	0

The table shows that the harmonic distortion rises due to the increasing power of the PFCU; this is because the resonant frequency is shifting towards lower frequencies, according to Equation (1), and resonant frequency can be calculated. The results of the resonant frequency calculations due to different powers of the PFCU are shown in Figure 10.
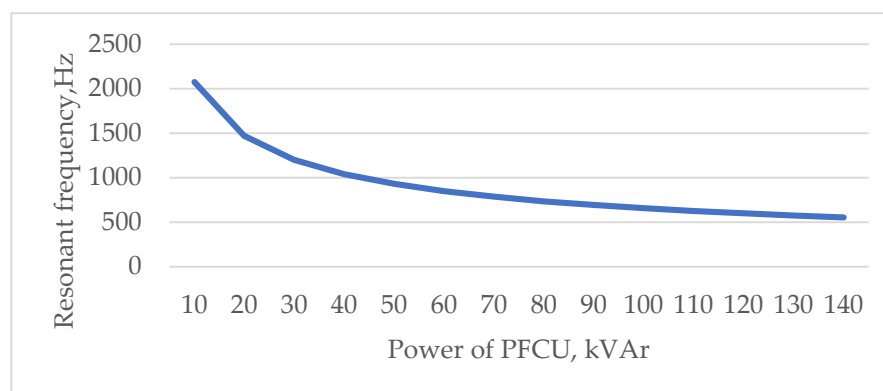

Figure 10. Resonant frequency versus different powers of the PFCU.

Recalculated current IB' allows us to find the most efficient scenario for the power transformer using Equation (10). The results are shown in Figure 11.
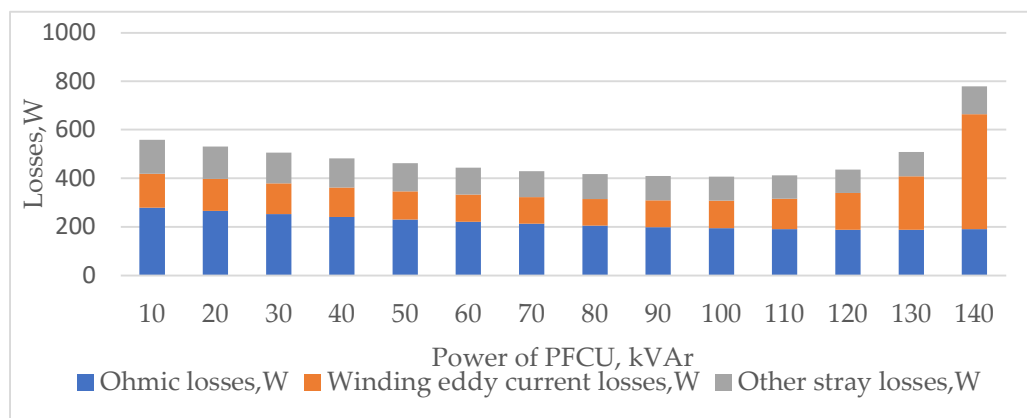
Figure 11. Calculated transformer losses due to different powers of PFCU.

The working regime of the PFCU with 100 kVAr of power leads to decreasing load losses of 48 percent compared to a fully compensated working mode of 140 kVAr. This leads to lower usage of the PFCU due to lower load and lower current harmonic quantities, which are shown in Figure 12.
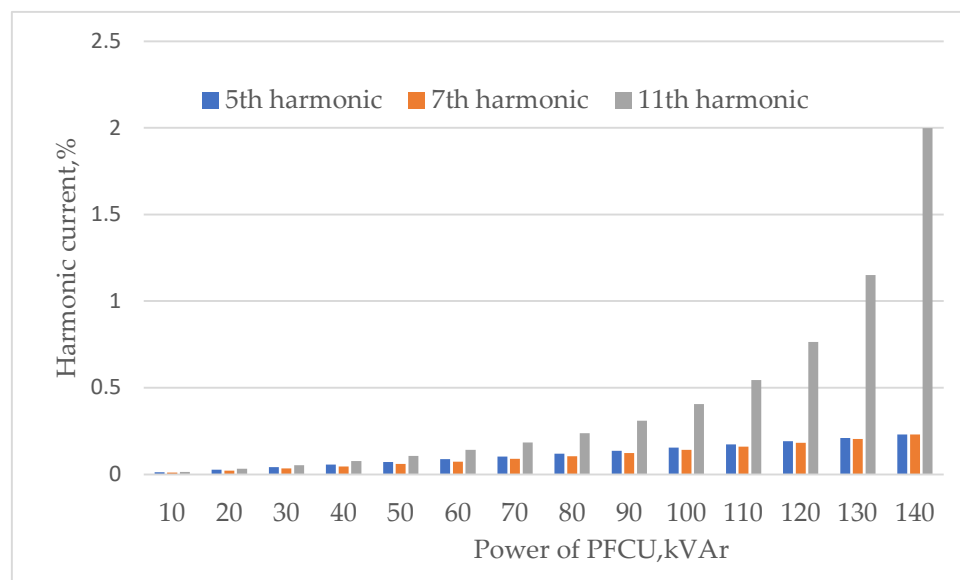

Figure 12. Changes in the harmonic current to branch due to different powers of PFCU.

4. Conclusions

Load-flow calculations, while more accurate, are typically executed using historical income data. However, this article establishes that real-time calculations prove to be more effective than load-flow simulations. This effectiveness is attributed to the constantly changing conditions, including, but not limited to, harmonic distortion, voltage levels, powers of the Power Factor Correction Units (PFCUs), and the dynamic behaviors of consumers. To implement the algorithm, PLC was chosen, due to its ability to collect data from power meters, PFCUs, and the possibility to control the PFCUs. To check the accuracy of the algorithm's results, they were compared with the simulation results of Power Factory applications and real measurements. The calculations resulted in a sufficient difference between the calculated values and modelled values, with a relative error of 0.024 percent. The accuracy of the algorithm was improved due to adding additional iterations, and the relative calculation error to simulated data decreased to 0.0108 percent. An additional Dijkstra algorithm was implemented to easier understand or visualize dangerous scenarios of resonance. The Dijkstra algorithm allows for identifying the conditions when some of

the branches have lower resistances than the grid connection point, and this means risk of resonance and highly distorted currents. The algorithm operates in a straightforward manner; it checks all the possible directions for the harmonic flow and chooses the path with lower resistance. In normal conditions, the lower resistance path is to the grid, except in resonance conditions. Using the first Kirchhoff's law, the calculation of current harmonic distributions was tested, assuming knowledge of the injected harmonic current. Subsequently, the calculations were reversed to ascertain the extent of harmonics flowing in medium voltage busbars when measurements were solely conducted on the low voltage side. This allowed us to implement the calculation of which power of the PFCU to use; how much harmonic current would be injected into the industrial branch instead of a grid; and to find the most efficient scenario of the PFCU, taking into account not only displacement power factor but harmonic distortion too. The results presented in the results section show that, even with a relatively small THD of current, the transformer losses are affected. The working regime of the PFCU with 100 kVAr of power leads to decreasing load losses of 48 percent compared to a fully compensated working mode of 140 kVAr. After evaluation of transformer losses with different PFCU powers, controlling the PFCU can be achieved only by using industrial communication protocols. The algorithm is easy to implement, and, in different hardware, the only limitations are due to support of the communication between devices. In many cases, only supporting serial communications as a Modbus RTU can be enough, due to its wide usage in industrial equipment. Communication requirements can also be different due to support protocols of EMSs for logging the measurement data. This algorithm should not overlap with the existing control because it is the main target just to control the target power factor, and, in most of the cases, this setting in the controller of the PFCU is fixed.

Future work will focus on calculations for bigger systems and evaluating the effects of voltage harmonic distortion.

Institutional Review Board Statement: Not applicable.

Informed Consent Statement: Not applicable.

Data Availability Statement: The data presented in this study are available on request from the corresponding author. The data are not publicly available due to involvement of the industry company.

Conflicts of Interest: The authors declare no conflict of interest.

References

1. Doytch, N.; Narayan, S. Does transitioning towards renewable energy accelerate economic growth? An analysis of sectoral growth for a dynamic panel of countries. *Energy* **2021**, *235*, 121290. [CrossRef]
2. Europe: Renewables in 2022 in Five Charts—And What to Expect in 2023. Available online: https://www.energymonitor.ai/renewables/europe-renewables-in-2022-in-five-charts-and-what-to-expect-in-2023/?cf-view (accessed on 24 November 2023).
3. Skamyin, A.; Shklyarskiy, Y.; Dobush, V.; Dobush, I. Experimental Determination of Parameters of Nonlinear Electrical Load. *Energies* **2021**, *14*, 7762. [CrossRef]
4. Europe Added 41.4 GW of New Solar in 2022. Available online: https://www.pv-magazine.com/2022/12/19/europe-added-41-4-gw-of-new-solar-in-2022 (accessed on 18 November 2023).
5. Liang, X. Emerging Power Quality Challenges Due to Integration of Renewable Energy Sources. *IEEE Trans. Ind. Appl.* **2016**, *53*, 855–866. [CrossRef]
6. Bhatt, P.K.; Patidar, N.P. Intelligent transformer tap controller for harmonic elimination in photovoltaic interfaced micro-grid network. *Eng. Optim.* **2022**, *55*, 1149–1167. [CrossRef]
7. Barelli, L.; Desideri, U.; Ottaviano, A. Challenges in load balance due to renewable energy sources penetration: The possible role of energy storage technologies relative to the Italian case. *Energy* **2015**, *93*, 393–405. [CrossRef]

8. Hamada, H.; Kusayanagi, Y.; Tatematsu, M.; Watanabe, M.; Kikusato, H. Challenges for a reduced inertia power system due to the large-scale integration of renewable energy. *Glob. Energy Interconnect.* **2022**, *5*, 266–273. [CrossRef]
9. Laimon, M.; Mai, T.; Goh, S.; Yusaf, T. System dynamics modelling to assess the impact of renewable energy systems and energy efficiency on the performance of the energy sector. *Renew. Energy* **2022**, *193*, 1041–1048. [CrossRef]
10. Owosuhi, A.; Hamam, Y.; Munda, J. Maximizing the Integration of a Battery Energy Storage System–Photovoltaic Distributed Generation for Power System Harmonic Reduction: An Overview. *Energies* **2023**, *16*, 2549. [CrossRef]
11. Baggini, A.B. *Handbook of Power Quality*; Wiley Online Library: Hoboken, NJ, USA, 2008; ISBN 9780470065617. [CrossRef]
12. Agha, A.H.; Luhach, A.K. Optimized Economic Loading of Distribution Transformers Using Minimum Energy Loss Computing. *Math. Probl. Eng.* **2021**, *2021*, 1–9. [CrossRef]
13. Rodrigues, C.E.M.; Tostes, M.E.d.L.; Bezerra, U.H.; Soares, T.M.; de Matos, E.O.; Filho, L.S.S.; Silva, E.C.d.S.; Rendeiro, M.F.; Moura, C.J.d.S. Technical Loss Calculation in Distribution Grids Using Equivalent Minimum Order Networks and an Iterative Power Factor Correction Procedure. *Energies* **2021**, *14*, 646. [CrossRef]
14. Tamboli, P.D.; Kulkarni, S.; Thosar, A.G. Energy Efficiency in Manufacturing Industry and Analysis of Industrial Motors. In Proceedings of the 2020 4th International Conference on Electronics, Communication and Aerospace Technology (ICECA), Coimbatore, India, 5–7 November 2020; pp. 170–175.
15. Driving down energy costs: A new report says energy efficiency is the best way for industries to cut spending and reduce emissions right now. In *Pit & Quarry*; North Coast Media, LLC: Cleveland, OH, USA, 2023; Volume 115, p. 46.
16. Zhang, Y.; Zhang, Y.; Chen, S.; Gong, S. How to reduce energy consumption by energy audits and energy management: The case of province Jilin in China. In Proceedings of the 2011 PICMET '11: Technology Management in the Energy Smart World (PICMET), Portland, OR, USA, 31 July–4 August 2011; pp. 1–5.
17. Dat, M.N.; Trung, K.D.; Minh, P.V.; Van, C.D.; Tran, Q.T.; Ngoc, T.N. Assessment of Energy Efficiency Using an Energy Monitoring System: A Case Study of a Major Energy-Consuming Enterprise in Vietnam. *Energies* **2023**, *16*, 5214. [CrossRef]
18. Akhtar, T.; Rehman, A.U.; Jamil, M.; Gilani, S.O. Impact of an Energy Monitoring System on the Energy Efficiency of an Automobile Factory: A Case Study. *Energies* **2020**, *13*, 2577. [CrossRef]
19. Pereira, L.; Nunes, N. Understanding the practical issues of deploying energy monitoring and eco-feedback technology in the wild: Lesson learned from three long-term deployments. *Energy Rep.* **2019**, *6*, 94–106. [CrossRef]
20. Sinvula, R.; Abo-Al-Ez, K.M.; Kahn, M.T. A Proposed Harmonic Monitoring System for Large Power Users Considering Harmonic Limits. *Energies* **2020**, *13*, 4507. [CrossRef]
21. Rinas, I.W.; Suartika, I.M.; Pemayun, A.A.M. Analysis of the Increase of Transformer Power Losses due to the Operation of Unbalanced Nonlinier Loads. *J. Electr. Electron. Inform.* **2018**, *2*, 38. [CrossRef]
22. Faiz, J.; Rezaeealam, B.; Mikhak-Beyranvand, M. Thermal analysis and derating of a power transformer with harmonic loads. *IET Gener. Transm. Distrib.* **2020**, *14*, 1233–1241. [CrossRef]
23. Can, B.; Ayan, O.; Silsupur, M.; Turkay, B.E. Harmonic Effects of Electric Vehicles on Low Voltage Distribution Transformers and Power Grid. In Proceedings of the 2018 2nd International Symposium on Multidisciplinary Studies and Innovative Technologies (ISMSIT), Ankara, Turkey, 19–21 October 2018; pp. 1–6.
24. Thango, B.A.; Jordaan, J.A.; Nnachi, A.F. Effects of Current Harmonics on Maximum Loading Capability for Solar Power Plant Transformers. In Proceedings of the 2020 International SAUPEC/RobMech/PRASA Conference, Cape Town, South Africa, 29–31 January 2020; pp. 1–5.
25. Morin, C.; Khodabakhchian, B. 765kV power transformer losses upon energizations: A comparison between field test measurements and EMTP-RV simulations. *Electr. Power Syst. Res.* **2014**, *115*, 35–42. [CrossRef]
26. Eslamian, M.; Vahidi, B. New Equivalent Circuit of Transformer Winding for the Calculation of Resonance Transients Considering Frequency-Dependent Losses. *IEEE Trans. Power Deliv.* **2014**, *30*, 1743–1751. [CrossRef]
27. Jiang, L.-M.; Meng, J.-X.; Yin, Z.-D.; Dong, Y.-X.; Zhang, J. Research on additional loss of line and transformer in low voltage distribution network under the disturbance of power quality. In Proceedings of the 2018 International Conference on Advanced Mechatronic Systems (ICAMechS), Zhengzhou, China, 30 August–2 September 2018; pp. 364–369.
28. Tan, Z.H.; Chua, K.H.; Lim, Y.S.; Morris, S.; Wang, L.; Tang, J.H. Optimal operations of transformers in railway systems with different transformer operation modes and different headway intervals. *Int. J. Electr. Power Energy Syst.* **2020**, *127*, 106631. [CrossRef]
29. Yan, X.; Yu, X.; Shen, M.; Xie, D.; Bai, B. Research on Calculating Eddy-Current Losses in Power Transformer Tank Walls Using Finite-Element Method Combined with Analytical Method. *IEEE Trans. Magn.* **2015**, *52*, 1–4. [CrossRef]
30. Özüpak, Y. Effect of Frequency on Eddy Losses of Transformers. *Int. J. Eng. Appl. Sci.* **2021**, *13*, 36–42. [CrossRef]
31. Thango, B.A.; Bokoro, P.N. Stray Load Loss Valuation in Electrical Transformers: A Review. *Energies* **2022**, *15*, 2333. [CrossRef]
32. Badri, J.A.; Riba, J.-R.; Garcia, A.; Trujillo, S.; Marzàbal, A. Transformer modelling considering power losses using an inverse Jiles-Atherton approach. *Int. J. Electr. Power Energy Syst.* **2023**, *154*, 109461. [CrossRef]
33. Avdeev, B.; Vyngra, A.; Chernyi, S. Improving the Electricity Quality by Means of a Single-Phase Solid-State Transformer. *Designs* **2020**, *4*, 35. [CrossRef]
34. Tavarov, S.S.; Zicmane, I.; Beryozkina, S.; Praveenkumar, S.; Safaraliev, M.; Shonazarova, S. Evaluation of the Operating Modes of the Urban Electric Networks in Dushanbe City, Tajikistan. *Inventions* **2022**, *7*, 107. [CrossRef]

35. Saxena, N.K.; Kumar, A. Analytical Comparison of Static and Dynamic Reactive Power Compensation in Isolated Wind–Diesel System Using Dynamic Load Interaction Model. *Electr. Power Compon. Syst.* **2015**, *43*, 508–519. [CrossRef]

36. Khatib, T.; Sabri, L. Grid Impact Assessment of Centralized and Decentralized Photovoltaic-Based Distribution Generation: A Case Study of Power Distribution Network with High Renewable Energy Penetration. *Math. Probl. Eng.* **2021**, *2021*, 5430089. [CrossRef]

37. Solomentsev, M.; Okeke, O.; Hanson, A.J. A Resonant Approach to Transformer Loss Characterization. In Proceedings of the 2022 IEEE Applied Power Electronics Conference and Exposition (APEC), Houston, TX, USA, 20–24 March 2022; pp. 596–603.

38. Frljić, S.; Trkulja, B.; Drandić, A. Eddy current losses in power voltage transformer open-type cores. *COMPEL—Int. J. Comput. Math. Electr. Electron. Eng.* **2023**, *42*, 1037–1049. [CrossRef]

39. Sima, L.; Miteva, N.; Dagan, K.J. A novel approach to power loss calculation for power transformers supplying nonlinear loads. *Electr. Power Syst. Res.* **2023**, *223*, 109582. [CrossRef]

40. Zi, C.; Guo, H.; Wang, S.; Sun, B. A study of on-line monitoring of electric energy balance of agricultural power grid under Internet of Things. In Proceedings of the Seventh International Conference on Mechatronics and Intelligent Robotics (ICMIR 2023), Kunming, China, 16–18 June 2023; Volume 12779, p. 127790Z.

41. Jagtap, S.; Rahimifard, S.; Duong, L.N.K. Real-time data collection to improve energy efficiency: A case study of food manufacturer. *J. Food Process. Preserv.* **2022**, *46*, e14338. [CrossRef]

42. Gan, L.; Huang, H.-H.; Li, L.; Xiong, W.; Liu, Z.-F. IoT-enabled energy efficiency monitoring and analysis method for energy saving in sheet metal forming workshop. *J. Cent. South Univ.* **2022**, *29*, 239–258. [CrossRef]

43. Benedetti, M.; Cesarotti, V.; Introna, V.; Serranti, J. Energy consumption control automation using Artificial Neural Networks and adaptive algorithms: Proposal of a new methodology and case study. *Appl. Energy* **2016**, *165*, 60–71. [CrossRef]

44. Ueno, T.; Sano, F.; Saeki, O.; Tsuji, K. Effectiveness of an energy-consumption information system on energy savings in residential houses based on monitored data. *Appl. Energy* **2006**, *83*, 166–183. [CrossRef]

45. Introna, V.; Cesarotti, V.; Benedetti, M.; Biagiotti, S.; Rotunno, R. Energy Management Maturity Model: An organizational tool to foster the continuous reduction of energy consumption in companies. *J. Clean. Prod.* **2014**, *83*, 108–117. [CrossRef]

46. Yin, S.; Yang, H.; Xu, K.; Zhu, C.; Zhang, S.; Liu, G. Dynamic real–time abnormal energy consumption detection and energy efficiency optimization analysis considering uncertainty. *Appl. Energy* **2022**, *307*, 118314. [CrossRef]

47. Rezaeealam, B.; Askary, S. Real-time monitoring of transformer hot-spot temperature based on nameplate data. *IET Gener. Transm. Distrib.* **2023**, *17*, 3140–3151. [CrossRef]

48. *C57.110™-2018*; IEEE Recommended Practice for Establishing Liquid-Immersed and Dry-Type Power and Distribution Transformer Capability When Supplying Nonsinusoidal Load Currents. IEEE: Piscataway, NJ, USA, 2018; pp. 1–68. [CrossRef]

49. Lu, G.; Zheng, D.; Zhang, Q.; Zhang, P. Effects of Converter Harmonic Voltages on Transformer Insulation Ageing and an Online Monitoring Method for Interlayer Insulation. *IEEE Trans. Power Electron.* **2021**, *37*, 3504–3514. [CrossRef]

50. Doolgindachbaporn, A.; Callender, G.; Lewin, P.; Simonson, E.; Wilson, G. Data Driven Transformer Thermal Model for Condition Monitoring. *IEEE Trans. Power Deliv.* **2021**, *37*, 3133–3141. [CrossRef]

51. Gulakhmadov, A.; Asanova, S.; Asanova, D.; Safaraliev, M.; Tavlintsev, A.; Lyukhanov, E.; Semenenko, S.; Odinaev, I. Power Flows and Losses Calculation in Radial Networks by Representing the Network Topology in the Hierarchical Structure Form. *Energies* **2022**, *15*, 765. [CrossRef]

52. Asanov, M.; Asanova, S.; Safaraliev, M.; Lyukhanov, E.; Tavlintsev, A.; Shelyug, S. Elementwise power losses calculation in complex distribution power networks represented by hierarchical-multilevel topology structure. *Prz. Elektrotech.* **2021**, *97*, 106–110. [CrossRef]

53. Shadab, S.; Revati, G.; Wagh, S.; Singh, N. Finite-time parameter estimation for an online monitoring of transformer: A system identification perspective. *Int. J. Electr. Power Energy Syst.* **2023**, *145*, 108639. [CrossRef]

54. Plienis, M.; Deveikis, T.; Jonaitis, A.; Gudžius, S. Design of IOT-Based Framework for Evaluation of Energy Efficiency in Power Transformers. *Energies* **2023**, *16*, 4358. [CrossRef]

55. Faiz, J.; Ghazizadeh, M.; Oraee, H. Derating of transformers under non-linear load current and non-sinusoidal voltage—An overview. *IET Electr. Power Appl.* **2015**, *9*, 486–495. [CrossRef]

56. Islam, M.; Sutanto, D.; Muttaqi, K.M. Protecting PFC Capacitors from Overvoltage Caused by Harmonics and System Resonance Using High Temperature Superconducting Reactors. *IEEE Trans. Appl. Supercond.* **2019**, *29*, 1–5. [CrossRef]

57. Motlagh, S.Z.T.; Foroud, A.A. Multiple harmonic sources identification including inverter-based distributed generations using empirical Fourier decomposition. *IET Gener. Transm. Distrib.* **2023**, *17*, 1932–1954. [CrossRef]

58. Khajeh, K.G.; Solatialkaran, D.; Zare, F.; Mithulananthan, N. An enhanced full-feedforward strategy to mitigate output current harmonics in grid-tied inverters. *IET Gener. Transm. Distrib.* **2020**, *15*, 827–835. [CrossRef]

59. Zhou, C.; Zhao, J.; Wang, H.; Yan, S.; Yan, D. Harmonic Analysis and Cancellation of Inverter Systems with Linear Phase-Shifting Transformer. *IEEJ Trans. Electr. Electron. Eng.* **2023**, *18*, 1617–1625. [CrossRef]

60. de Jesus, V.M.R.; Cupertino, A.F.; Xavier, L.S.; Pereira, H.A.; Mendes, V.F. Operation Limits of Grid-Tied Photovoltaic Inverters with Harmonic Current Compensation Based on Capability Curves. *IEEE Trans. Energy Convers.* **2021**, *36*, 2088–2098. [CrossRef]

61. Sriyono; Khayam, U. Suwarno Evaluating the Inter-Resonance Characteristics of Various Power Transformer Winding Designs. *IEEE Access* **2021**, *9*, 54649–54656. [CrossRef]

62. Geth, F.; Van Acker, T. Harmonic optimal power flow with transformer excitation. *Electr. Power Syst. Res.* **2022**, *213*, 108604. [CrossRef]
63. Sumper, A.; Baggini, A. *Electrical Energy Efficiency: Technologies and Applications*; John Wiley & Sons, Incorporated: Hoboken, NJ, USA, 2012. Available online: https://ebookcentral.proquest.com/lib/ktu-ebooks/detail.action?docID=875759 (accessed on 20 November 2023).
64. Lemieux, G. Power system harmonic resonance-a documented case. *IEEE Trans. Ind. Appl.* **1990**, *26*, 483–488. [CrossRef]
65. Deshpande, R.P. *Capacitors*, 1st ed.; McGraw-Hill Education: New York, NY, USA, 2015. Available online: https://www.accessengineeringlibrary.com/content/book/9780071848565 (accessed on 1 November 2023).
66. Nafisi, A.; Rezvani, M.; Arababadi, R.; Esmaeili, S. Harmonic Resonance Assessment Based on Field Measurements Data in an Industrial Plant. In Proceedings of the 2020 19th International Conference on Harmonics and Quality of Power (ICHQP), Dubai, United Arab Emirates, 6–7 July 2020; pp. 1–6.
67. Boonseng, C.; Chompoo-Inwai, C.; Kinnares, V.; Nakawiwat, K.; Apiratikul, P. Failure analysis of dielectric of low voltage power capacitors due to related harmonic resonance effects. In Proceedings of the 2001 Winter Meeting of the IEEE Power Engineering Society, Columbus, OH, USA, 28 January–1 February 2001; Volume 3, pp. 1003–1008.
68. Hofmann, W.; Schlabbach, J.; Just, W. *Reactive Power Compensation*; Wiley: Hoboken, NJ, USA, 2012; ISBN 9780470977187. [CrossRef]
69. Bayliss, C. *Transmission and Distribution Electrical Engineering*, 4th ed.; Elsevier: Amsterdam, The Netherlands, 2011. [CrossRef]